

WSA₁: a 3D-Centric World-Spatial-Action Model for Generalizable Robot Control

Jiahao Jiang Jianing Zhang Zhenhan Yin Ruidong Chen Sen Wang Zhaoshu Yu
 Pengpeng Zeng Xiaofeng Cao Xuanhan Wang[†]◇ Jingkuan Song[†]◇ Heng Tao Shen[†]◇
 Tongji University; Shanghai Innovation Institution; Shanghai Magic; Koala Uran

Project Page: <https://github.com/zaleni/WSA>

[†]Project Leader ◇Corresponding Author

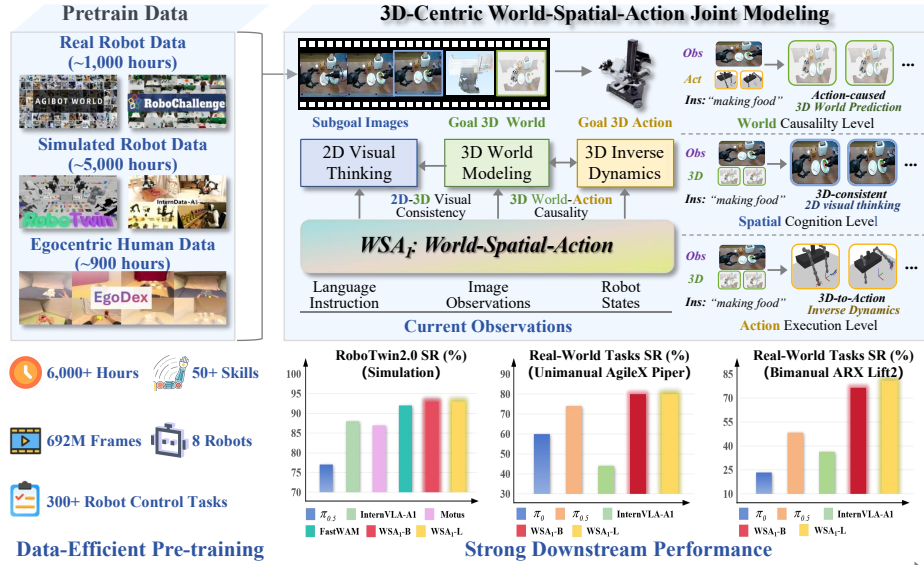


Figure 1: WSA₁: A generalizable robot foundation model built upon 3D-centric world-spatial-action modeling, achieving highly competitive manipulation performance across diverse simulated and real-robot benchmarks using only 6K hours of pre-training data.

Abstract

Recent advances in embodied AI have established robot foundation models (RFMs) as the dominant approach for generalist robotic systems to date. By leveraging imitation learning on extensive robot demonstrations, RFMs have achieved impressive capabilities in mapping visual observations and language instructions to continuous robotic actions. However, current RFMs lack an inherent ability to reason about physical dynamics and the causal effects of robot behaviors on the 3D physical world. This creates a fundamental mismatch between 2D-centric visual perception and 3D-centric embodied interaction, severely limiting the generalization ability of RFMs in real-world tasks. To address this gap, we present WSA₁, a novel RFM built upon proposed 3D-Centric World-Spatial-Action modeling paradigm. It not only learns 3D world-aware visual thought for future robot behaviors, but also models mutual constraints between 3D world state transitions and robotic actions to enhance behavior generalization. Notably, WSA₁ achieves highly data-efficient pre-training with 6k hours of expert demonstration data (only 1k hours from real robot), while delivering competitive manipulation performance (93% success rate) on RoboTwin2.0 simulation benchmark and achieving +20% average boosted performance over state-of-the-art RFMs on real-world robot control tasks. These results reveal that generalizable RFM can be attained without large-scale real robot data when paired with 3D-centric world-action joint modeling, which offers a practical and affordable pathway to generalist robotic systems.

Contents

1	Introduction	3
2	Related Work	4
3	Methodology	5
3.1	Problem Definition and Notation	5
3.2	Model Architecture	6
3.3	World-Spatial-Action Joint Modeling	7
3.4	Pre-training Data Recipe	8
4	Experiments	9
4.1	Experimental Setup	9
4.2	Main Results on Real-World Tasks	10
4.3	Main Results on Simulation Benchmark	11
4.4	Ablation Study	12
4.5	Qualitative Analysis	14
5	Conclusion	15

1 Introduction

Creating versatile robots to match or exceed human-level physical intelligence has long been a core pursuit in embodied AI. Cognitive science and neuroscience research reveals that human physical intelligence relies critically on our innate ability to construct and maintain an internal 3D spatial model of the world [37]. This mental model enables us to parse the 3D structure of our surroundings, predict how our actions will causally alter the world state, and plan and execute dexterous motor interactions accordingly [12]. In short, humans achieve flexible physical interaction through the co-modeling of world, space, and action in a unified 3D representation. This 3D-centric capability of world-spatial-action co-modeling is equally vital for generalist robots, given that all physical interactions in the real world inherently unfold in 3D space and obey fundamental physical laws [13, 15]. Thus, developing a robot foundation model that can capture essential relationships between 3D world evolution and robot behaviors, is the critical breakthrough needed to unlock the full potential of embodied AI.

In recent years, multi-modal large models [11, 3, 45, 35] have achieved remarkable progress and, meanwhile, demonstrated a promising technical roadmap toward beyond human-level intelligence through training on web-scale data. Following this direction, modern robot foundation models have gradually evolved into two typical paradigms: Vision-Language-Action (VLA) models [24, 50, 36, 31, 7, 6, 17, 48] and World Action Models (WAM) [4, 27, 9, 19, 44, 41, 16]. VLA models construct semantic-centric robotic policies by augmenting pre-trained vision-language models (VLMs) with a lightweight action expert. This design allows VLAs to inherit powerful open-world visual understanding capabilities from pre-trained VLMs, while the appended action expert generates robot actions conditioned on semantic-level visual comprehension, following an "understand-then-execute" paradigm. In contrast, WAM learns imagination-centric robot policies based on a predictive video generation model that acts as a vision planner. Based on this "imagine-then-execute" paradigm, its action expert functions as an inverse dynamics model, which generates robotic control signals corresponding to the planned visual frames.

Despite the impressive progress of current VLAs and WAMs, two fundamental challenges still impede their generalization to real-world scenarios. **First**, from a model paradigm perspective, both VLAs and WAMs lack an explicit mechanism for jointly modeling the 3D world dynamics and mutual constraints between robot actions and world changes. The absence of explicit 3D world-action mutual constraints renders them unreliable in real-world tasks that require 3D spatial cognition and robust adaptation to environmental changes. **Second**, in terms of model training, the major optimization strategy for robot foundation models is the imitation learning, which heavily depends on large-scale real-world expert demonstration data. Acquiring such data at scale is prohibitively expensive and labor-intensive [5]. This data scarcity further prevents models from learning the generalizable physical commonsense behind demonstrations, which is essential for developing generalist robots that can adapt to unseen scenarios [5, 4]. These challenges motivate us to study a significant question:

How can we construct a data-efficient modeling paradigm that enables robots to jointly model interdependencies between 3D world evolution and physical behaviors from demonstrations, thereby overcoming the generalization bottleneck of naive imitation via learned transferable world-action priors?

In this work, we present **WSA₁**, a novel robot foundation model built on 3D-centric World-Spatial-Action joint modeling paradigm. As illustrated in Figure 3, the WSA breaks the inherent limitations of prevailing paradigms via unification of three learning tasks. First, **at the world causality level**, it explicitly models action-caused 3D world prediction, endowing a robot with the ability to capture the causal consequence of robot behaviors on 3D world. Second, **at the spatial cognition level**, it enables 3D-consistent 2D visual thinking, which empowers a robot to dynamically adjust visual plan as the 3D world changes. Third, **at the action execution level**, it learns a 3D inverse dynamics model that maps the planned 3D world state transitions to executable robot actions, fully closing the loop between 3D spatial world modeling and real-world interaction. This integrated closed-loop design allows a robot to not only generate goal-directed actions, but also predict causal consequences of its actions on 3D world and dynamically adjust its behavior accordingly. In summary, our main contributions are three-fold:

- **A 3D-Centric World-Spatial-Action Modeling Paradigm.** We propose WSA, a novel robot learning paradigm that unifies three complementary learning objectives within a single shared latent space: predictive 3D world modeling, 3D-consistent 2D visual thinking, and 3D inverse

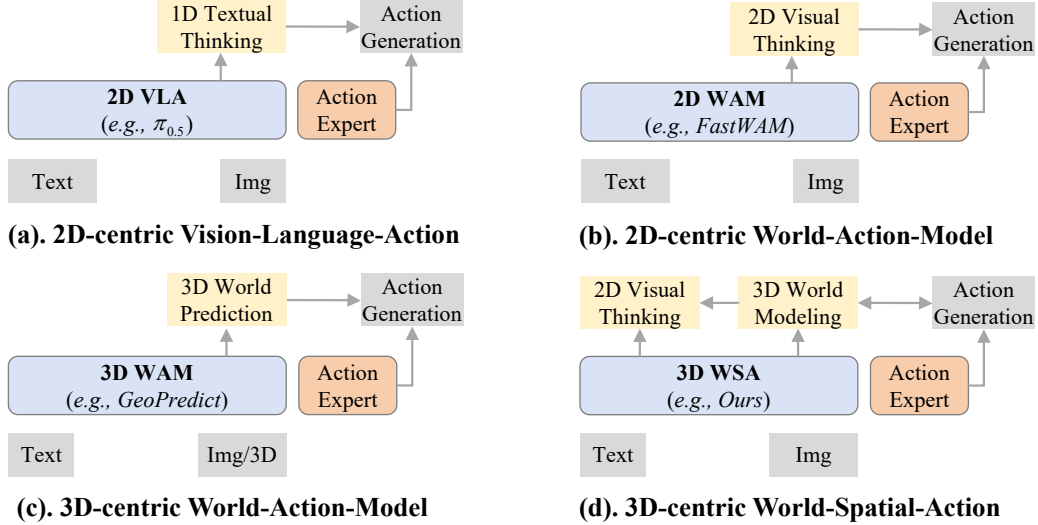


Figure 2: **Prevailing Modeling Paradigms:** (a) 2D-centric VLA models unidirectional mappings from visual semantics to physical actions; (b) 2D-centric WAM jointly models 2D visual dynamics and physical actions; (c) 3D-centric WAM jointly models 3D scene geometry and physical actions; (d) Our 3D-centric WSA jointly models 3D world dynamics, physical actions, and their interdependencies.

dynamics. By incorporating world-action mutual constraints, WSA addresses the generalization limitations of prevailing VLA and WAM paradigms.

- **A Generalizable Robot Foundation Model.** We instantiate the WSA paradigm with two model scales, WSA₁-B (3B) and WSA₁-L (6B). Both are built on a Mixture-of-Transformers architecture with three complementary experts. A bidirectional attention mechanism is proposed to enforce world-action consistency and enable joint learning across all three objectives in a unified framework.
- **Data-Efficient Generalization with Empirical Validation.** Pre-trained on only 6,000 hours of heterogeneous demonstration data (including just 1,000 hours of real-robot data), WSA₁ models achieve state-of-the-art performance among open-source models on RoboTwin2.0 (93% SR) and deliver an average +20% improvement over baselines across real-world manipulation tasks, demonstrating that 3D-centric world-spatial-action joint modeling enables data-efficient learning of generalizable manipulation skills.

2 Related Work

The core goal of robot foundation models (RFMs) is to establish a robust, stable multi-modal mapping from robot observations and task instructions to executable robot actions [46, 43]. As illustrated in Figure 2, mainstream research on RFMs has converged into two dominant paradigms: Vision-Language-Action models (VLAs) and World-Action-Models (WAMs). In the following sections, we provide a systematic literature review of these two research directions.

Vision-Language-Action: As the most widely adopted paradigm for robot manipulation, VLA models [36, 7, 6, 39, 48] are generally built on pretrained vision-language models. By inheriting rich semantic priors from VLMs [11, 3], they successfully transfer open-world visual-semantic knowledge to the physical robot domain via end-to-end fine-tuning on robot demonstration data. Early representative works such as RT-2 [50] and OpenVLA [17] adopt an autoregressive strategy, which discretizes continuous robot actions and formulates policy learning as a sequence modeling task. To address the limitation of discrete tokenization in fine-grained continuous control, recent state-of-the-art works [7, 6, 5] have shifted to generative frameworks based on conditional flow matching, which directly model the continuous-valued action, significantly improving the precision and stability of robot control. In addition, several works [49, 29] augment VLA with 3D geometry priors by incorporating extra 3D information such as depth or 3D gaussian splatting, demonstrating the effectiveness of 3D representation in robot learning. However, mainstream VLA policies are

essentially reactive frameworks that make decisions based only on current observations, lacking predictive planning and 3D causal reasoning capabilities, which makes them unreliable in real-world manipulation tasks that require 3D dynamics modeling.

World-Action-Model: In a different line from VLAs, WAMs follow the chain-of-thought philosophy and formulate robot policies as an imagine-then-execute procedure. Guided by this principle, numerous works [27, 41, 16, 44, 25] start with video models, inheriting rich commonsense knowledge from large-scale video generation pre-training. They then use these video models as world dynamics simulators, enhancing the reliability of robot foundation models via co-training of future frame prediction and action generation. For example, Motus [4] demonstrates that explicitly modeling future frame prediction significantly improves the generalization of robot manipulation, while Fast-WAM [44] proves that improved manipulative generalization comes from the co-learning rather than explicit video prediction. Furthermore, recent efforts [28, 47, 20] have further extended WAM paradigm to 3D space by modeling future geometry prediction. For instance, GeoPredict [28] leverages predictive kinematics and 3D Gaussian geometry to improve the manipulation performance, and PointWorld [15] scales 3D world models for in-the-wild robotic manipulation. However, existing 3D WAMs still follow a unidirectional "predict-then-execute" pipeline, failing to unify 3D world dynamics modeling and inverse dynamics into a single latent space for bidirectional causal learning. They cannot explicitly model how robot actions affect 3D space evolution and, in turn, how 3D space changes should guide action generation, which is the core focus of our work.

Compared with prior studies, our work is most closely related to WAMs but takes a further step: instead of directly co-learning video generation and robot control, our method unifies action-caused 3D world modeling and 3D inverse dynamics into a single model. This mechanism enables our model to exploit the intrinsic causal consistency: it not only learns how 3D robot actions affect the evolution of the 3D world but also determines the appropriate action plan given variations in the 3D world.

3 Methodology

In this section, we first formalize the robot control problem in Section 3.1. We then introduce the overall architecture of WSA₁ in Section 3.2, followed by detailed learning objectives of the 3D-centric world-spatial-action joint modeling in Section 3.3. Finally, we present the pre-train data recipe in Section 3.4.

3.1 Problem Definition and Notation

In the context of robot control, the goal of embodied foundation model is to learn a robot policy that predicts next robot actions from current observations. Formally, at each timestep t , the observations include task instruction termed l , visual observation denoted as v_t , and robot proprioception termed s_t . In general, the robot action is a H -step chunk termed $A_t := (\mathbf{a}_{t+1}, \dots, \mathbf{a}_{t+H})$, a short-term action trajectory with a sequence of end-effector pose or joints of a robot in next H timesteps. To train a robot policy π_θ parameterized by θ on diverse robot demonstrations \mathcal{D}_{dem} , it is required to maximize the standard likelihood objective:

$$\max_{\theta} \mathbb{E}_{(v_t, s_t, A_t, l) \sim \mathcal{D}_{\text{dem}}} \log \pi_\theta(A_t | v_t, s_t, l). \quad (1)$$

As illustrated in Figure 2, previous works formulate robot control problem as vision-language-action or world-action policy, which can be regarded as a joint distribution derived from the standard objective.

2D Vision-Language-Action Policy. The 2D-centric VLA aims to directly predict executable actions conditioned on the current 2D observation $\mathbf{O}_t := \{v_t, s_t, l\}$. It learns 2D semantic-action unidirectional causality, which is formulated as a posterior distribution:

$$\mathbf{A}_t \sim p(a_{t+1:t+H} | v_t, s_t, l). \quad (2)$$

2D World-Action Policy. The 2D-centric WAM couples predictive visual generation with next action generation, which jointly predicts executable actions and N subgoal images $\mathbf{V}_t := (v_{t+1}, \dots, v_{t+N})$ from the current observation \mathbf{O}_t . It learns 2D world-action unidirectional causality, which can be

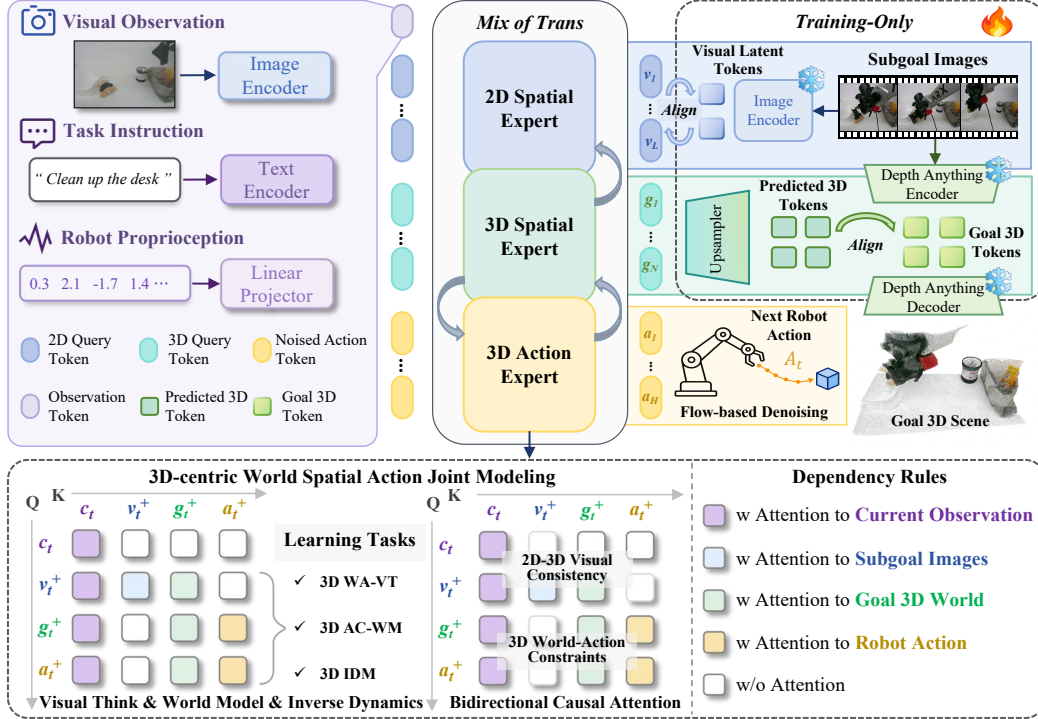


Figure 3: Overview of WSA_1 . It adopts a Mixture-of-Transformers structure with three complementary experts: a 2D Spatial Expert for 3D world-aware visual thinking, a 3D Spatial Expert for action-caused 3D world prediction, and a 3D Action Expert for 3D inverse dynamics modeling. A bidirectional causal attention mechanism enforces dependency rules to unify 3D-consistent visual thinking and world–action mutual constraints within a shared latent space.

formulated as a joint prediction distribution:

$$\mathbf{A}_t \sim p(a_{t+1:t+H}, v_{t+1:t+N} \mid v_t, s_t, l). \quad (3)$$

3D World-Action Policy. Instead of modeling 2D world-action joint distribution, the 3D-centric WAM focuses on the unidirectional causality between evolution of scenes and robot action in 3D space. Specifically, given 2D observation \mathbf{O}_t and 3D observation g_t , it learns to predict K future scenes of 3D world $\mathbf{G}_t := (g_{t+1}, \dots, g_{t+K})$ for robot control. Formally, this models a joint prediction distribution as follows:

$$\mathbf{A}_t \sim p(a_{t+1:t+H}, g_{t+1:t+K} \mid g_t, v_t, s_t, l). \quad (4)$$

3D World-Spatial-Action Policy. Different from previous VLA and WAM paradigms that rely on unidirectional mappings, we formulate robot control as world-spatial-action joint learning that captures the interdependencies among 3D world dynamics, visual cognition, and physical actions. Specifically, it jointly learns three complementary conditional distributions that impose consistency constraints among 3D world model, 2D visual thinking, and 3D inverse dynamics:

$$\underbrace{p(g_{t+1:t+K} \mid a_{t+1:t+H}, \mathbf{O}_t)}_{\text{Action-conditioned 3D World Model}}, \quad \underbrace{p(v_{t+1:t+N} \mid g_{t+1:t+K}, \mathbf{O}_t)}_{\text{2D visual thinking}}, \quad \underbrace{p(a_{t+1:t+H} \mid g_{t+1:t+K}, \mathbf{O}_t)}_{\text{3D Inverse Dynamics}} \quad (5)$$

These three distributions correspond to the three levels of the WSA framework: the world causality level (predicting how actions shape the 3D world), the spatial cognition level (grounding visual predictions in 3D geometry), and the action execution level (generating motor commands from 3D world states).

3.2 Model Architecture

Inspired by the recent works [4, 6], WSA_1 is built upon a unified multi-modal transformer, which leverages mixture-of-transformer (MoT) architecture to enable seamless integration of 2D visual

generation, future 3D prediction and robot action generation. As illustrated in Figure 3, it involves three major components: 2D spatial expert, 3D spatial expert and 3D action expert.

2D Spatial Expert (2D-SE): Given a human instruction, generating 3D goal-directed visual changes in 2D space enhances understanding of world dynamics. The 2D-SE $f_{2D}(\cdot)$ serves as the world-aware visual thinking branch of WSA₁. It is initialized from a pre-trained vision-language model such as QWen3-VL [2] or Wan2.2 [32], thereby inheriting strong vision-language priors. The goal of 2D-SE is to predict future 2D visual dynamics to reach the target state of the 3D world. Specifically, it predicts highly abstracted tokens $h_v = f_{2D}(O_t, G_t)$ for subgoal images, instead of RGB pixels. This design enhances visual understanding capability of the 2D-SE, as it is required to focus on essential features of an image rather than redundant pixel information.

3D Spatial Expert (3D-SE): Given a sequence of executable robot actions, predicting evolution of world dynamics in 3D space reflects causal effect of the robot behavior. Under this context, the 3D-SE $f_{3D}(\cdot)$ conducts an internal mechanism for 3D causal world modeling. To capture essential feature of 3D scenes, the 3D-SE predicts latent representations $h_g = f_{3D}(O_t, A_t)$ for subgoal 3D scenes. We construct it with a transformer-based module of the same depth as 2D-SE, thereby the architecture of 3D-SE can be directly derived from that of 2D-SE.

3D Action Expert (3D-AE): Given a demonstration of 3D space evolution, predicting next robot action tells why and how robot to behave in 3D space. The 3D-AE $f_{act}(\cdot)$ aims to predict a full action chunk conditioned on both current observations and future 3D latent representations. Specifically, we instantiate 3D-AE as denoising diffusion transformer. Given noisy actions $\hat{A}_t = \tau A_t + (1 - \tau)\omega$, where $\omega \sim \mathcal{N}(0, 1)$ and $\tau \in [0, 1]$, it employs iterative cross-attention and denoising procedure to predict latent action representations $h_{act} = f_{act}(O_t, G_t, \hat{A}_t)$. This yields a 3D inverse dynamics formulation, where 3D-AE maps predicted 3D latent evolution back to executable action.

3D-centric World-Action Causal Attention: Three experts are coupled within the mixture-of-transformer architecture via a shared attention mechanism. Formally, let h_t denote tokens of current observation, which are extracted via 2D-SE. As illustrated in Figure 3, we adopt a 3D-centric causal attention mechanism, which defines the following dependency rules: (1) All predicted tokens (h_v, h_g, h_{act}) can attend to the current observation tokens h_t , ensuring all predictions are grounded in the current state of the robot and the environment. (2) The visual tokens of future subgoal images h_v can attend to the 3D scene tokens h_g , encouraging the model to learn 2D-3D visual consistency and ground semantic visual predictions in physically consistent 3D geometry. (3) The 3D scene tokens h_g and action tokens h_{act} have full bidirectional attention access to each other, enabling joint learning of action-conditioned 3D dynamics prediction and 3D scene-aware action generation. This bidirectional attention is the key to modeling world-action interdependence of the WSA paradigm, as it reflects a causal inductive bias that drives the model to capture how actions shape world evolution and how world states inform action generation, rather than merely learning correlational mappings.

In this work, we implement two variants of WSA₁ equipped with different backbone architectures: WSA₁-B, a base model initialized from the pretrained Qwen3-VL-2B with a total of 3B parameters; and WSA₁-L, a large variant built on the pretrained Wan2.2-5B with a total of 6B parameters.

3.3 World-Spatial-Action Joint Modeling

Inspired by the internal model theory in cognitive neuroscience [37, 12], the WSA paradigm is designed to mirror three core computational principles of the human brain: 1) 3D spatial grounding of perception, 2) forward predictive modeling of action consequences, and 3) inverse motor control for goal-directed behavior. These three principles correspond to following three levels of the WSA framework, respectively.

3D World-Aware Visual Thinking (3D WA-VT). Analogous to the brain’s ability to form mental imagery of future scenes [18], the 2D Spatial Expert learns to predict 3D-grounded visual subgoals. Therefore, we adopt a MSE loss over the predicted visual tokens, to minimize the discrepancy between the predicted subgoal image tokens and the ground-truth tokens extracted via pre-trained tokenizer. Formally, the loss is defined as:

$$\mathcal{L}_{2D} = \mathbb{E}_{(O_t, G_t, V_t) \sim \mathcal{D}_{dem}} \|f_{2D}(O_t, G_t) - f_{enc}(V_t)\|_2^2, \quad (6)$$

where $f_{enc}(\cdot)$ denotes a pre-trained VAE-based tokenizer (e.g., COSMOS [1]).

Action-Conditioned 3D World Modeling (3D AC-WM). We adopt MSE loss over the predicted 3D scene latent representations, to minimize the error between the predicted future 3D states and the ground-truth 3D geometric states from the demonstration data. The loss is formalized as:

$$\mathcal{L}_{3D} = \mathbb{E}_{(O_t, A_t, G_t) \sim \mathcal{D}_{dem}} \|f_{3D}(O_t, A_t) - f_g(G_t)\|_2^2, \quad (7)$$

where $f_g(\cdot)$ denotes a pre-trained 3D foundation model, e.g., Depth-Anything [21]. This corresponds to the forward internal model in motor control theory [37], which predicts how motor actions will alter the state of the environment.

3D Inverse Dynamics Modeling (3D IDM). Following previous works [28, 6], we adopt flow matching loss [22] for continuous action generation. This loss minimizes the error between the predicted flow field and the ground-truth one, conditioned on the current observation and the 3D scene state evolution. The loss is defined as:

$$\mathcal{L}_{ACT} = \mathbb{E}_{(O_t, G_t, A_t) \sim \mathcal{D}_{dem}} \left\| \omega - A_t - f_{act}(O_t, G_t, \hat{A}_t) \right\|_2^2. \quad (8)$$

This trains 3D-AE to predict flow field ($\omega - A_t$), thereby facilitating coherent action generation. The overall learning objective is the sum of the three losses:

$$\mathcal{L}_{total} = \mathcal{L}_{2D} + \mathcal{L}_{3D} + \mathcal{L}_{ACT}. \quad (9)$$

We adopt two-stage strategy to optimize the WSA₁: pre-training on diverse data sources to acquire real-world behavior priors in first stage; post-training on specific manipulation tasks to adapt learned priors to target embodiment in second stage. Different from previous works [9, 4], WSA models are trained by co-learning of three capabilities in both pre-training and post-training stage.

3.4 Pre-training Data Recipe

High-quality embodied data is the cornerstone of pre-training generalizable embodied foundation models that can acquire versatile manipulation skills for flexible real-world robot control. Existing RFMs [7, 19, 26] typically rely on tens of thousands of hours of robot demonstration data to achieve broad generalization, with real-robot data constituting a major portion of their pre-training corpora. However, large-scale real-robot data collection remains prohibitively expensive and operationally challenging due to the cost and safety constraints of human-robot teleoperation [5]. To mitigate this bottleneck, alternative embodied data sources such as simulation data and egocentric human data have emerged as critical complements. This gives rise to a multi-sourced data pyramid [5, 4], where data quantity decreases from the bottom to the top. It suggests that each data layer exhibits distinct, complementary strengths and inherent limitations, and no single data source alone can support the development of generalizable embodied foundation model: human data (at the bottom of the pyramid) provides the "what" and "why" of tasks, simulation robot data (at the middle) offers the "how" for robot control, and real-world robot data (at the top) bridges the "reality gap" between simulation and physical environments [42]. No single data source alone can support the development of truly generalizable robot foundation models. Their synergistic integration is therefore not merely beneficial but essential for pre-training robust, versatile, and human-aligned robot foundation models that can generalize across tasks, platforms, and physical environments. Building on this insight, we argue that data diversity is the key to data-efficient robot foundation model pre-training. Accordingly, as illustrated in Table 1, we pre-train the model on a carefully curated mixture of heterogeneous data sources, totaling only 6,000 hours of demonstration data. The details of data recipe are provided below:

- **Simulation data:** We collect simulated synthetic data from InternData-A1 [33] and RoboTwin2.0 [10], providing diverse and low-cost manipulation trajectories for learning scene dynamics, object interaction, and coordinated control.
- **Human data:** We include egocentric human manipulation videos from EgoDex [14], which provide rich hand-object interaction priors and further enhance the model’s understanding of manipulation behaviors and scene evolution.

- **Real-world data:** The real-world robot data are drawn from RoboChallenge [38] and AgiBot-World [8], which help reduce the sim-to-real gap and improve robustness in physical environments.

The mixture of data sources covers 8 different robot embodiments and 300+ robot control tasks, including 50+ atomic manipulation skills such as grasping and placing. We show in subsequent experiments that this diverse data recipe, combined with our 3D-centric joint modeling paradigm, enables competitive generalization performance with significantly less real-robot data than existing approaches.

Table 1: Data mixture and training objectives used for pretraining. A checkmark indicates that the corresponding loss is enabled, while “-” indicates that the loss is masked out.

Data source	Type	Num. frames	Num. tasks	Sampling weight	\mathcal{L}_{2D}	\mathcal{L}_{3D}	\mathcal{L}_{ACT}
InternData-A1 [33]	Sim.	396M	70	0.47	✓	✓	✓
RoboTwin [10]	Sim.	17M	50	0.07	✓	✓	✓
AgiBot-World [8]	Real	206M	217	0.17	✓	✓	✓
RoboChallenge [38]	Real	5M	30	0.19	✓	✓	✓
EgoDex [14]	Human	68M	194	0.10	✓	✓	-

4 Experiments














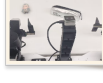
In this section, we introduce comprehensive evaluation experiments, which are conducted to explore the following questions: 1) How does proposed WSA₁ perform compared to existing VLA/WAM models across multiple benchmarks and embodiments? 2) How does the design choice in proposed WSA paradigm contribute to robot learning performance? Next, we first present experimental setup. Then, we demonstrate the merit of WSA₁ through a comparison with state-of-the-arts on both simulation and real-world tasks. Finally, we conduct ablation studies to illustrate major properties of proposed WSA paradigm.

4.1 Experimental Setup

Real-robot setup Real robot experiments are conducted with two robots: (1) Unimanual AgileX PiPER with three cameras and 7-DoF robotic arm; (2) Bimanual ARX Lift2 with three cameras and two 7-DoF robotic arms. To ensure diversity of robot behaviors in real-world scenario and investigate cross-embodiment generalization, we design 7 tabletop manipulation tasks. For each task, objects are randomly initialized within the workspace to evaluate model’s generalization capability across object position, orientation, and scene layout. The robot receives language instructions and visual observations as input, and predicts continuous action chunks for closed-loop execution. For testing, we adopt two metrics for comprehensive evaluation of RFMs: (1) Success Rate (SR), the proportion of rollouts in which the task is successfully completed. (2) Completeness (C), the proportion of rollouts in which the sub-task is completed.

Simulation setup We adopt RoboTwin-2.0 [10] and LIBERO [23] for evaluation in simulation environment. RoboTwin platform is setup with easy and hard modes, where the former offers clean environment without any distractor factor and the latter conduct domain randomization with background changes and distracted objects. Following official protocol [10], 27500 demonstrations (2500 for clean, 25000 for hard) are adopted for model fine-tuning. In addition, we adopt multi-task test setting (i.e., train for once, test for all tasks) to evaluate how much versatility of each model attain. During testing, success rate is adopted as the evaluation metric following the official protocol. The Libero is designed to assess four robot capabilities: spatial understanding, object-level manipulation, goal-conditioned execution, and long-horizon reasoning. Each suite contains 10 tasks, with 50 human-teleoperated demonstrations.

Table 2: Real-robot experimental setup and task details. Trajectory Num./Time denotes the number of collected demonstration trajectories and the total data collection time in minutes.

Initial	Finished	Robotic Embodiment	Trajectory Num. / Time	Task Description
		Unimanual: AgileX PiPER (7-DoF)	30 / 21 min	RGB Block Sorting: Position red block, green block, and blue block from left to right in the specified sequence.
		Unimanual: AgileX PiPER (7-DoF)	50 / 39 min	Object Organization: Tidy up the table by sorting the toys, stationery, and trash into their designated containers.
		Bimanual: ARX Lift2 (14-DoF)	30 / 5 min	Trash Cleaning: Pick up the trash with the nearest gripper, hand it over to the other gripper, and place it into the trash bin.
		Bimanual: ARX Lift2 (14-DoF)	30 / 4 min	Pen Holder Placement: Pick up the stationery on the table and place it into the pen holder.
		Bimanual: ARX Lift2 (14-DoF)	30 / 4 min	Toy Box Organization: Pick up the toys from the desktop, place them into the toy box, and arrange them neatly inside.
		Bimanual: ARX Lift2 (14-DoF)	90 / 31 min	Sweep Trash: Sweep the trash into the dustpan using a broom.
		Bimanual: ARX Lift2 (14-DoF)	30 / 8 min	Unzip Pencil Bag: Grasp the pencil bag, unzip it, and place it back onto the tabletop.

4.2 Main Results on Real-World Tasks

Real-world Evaluation Tasks As illustrated in Table 2, the real-world benchmark consists of 7 representative tabletop scenarios: RGB Block Sorting, Object Organization, Trash Cleaning, Pen Holder Placement, Toy Box Organization, Sweep Trash and Unzip Pencil Bag. These tasks require the robot to perceive cluttered scenes, interact with objects of different categories and spatial layouts, and complete multi-step manipulation behaviors such as grasping, placing, pushing, and sweeping. Compared with simple pick-and-place tasks, these scenarios place higher demands on spatial reasoning, long-horizon execution, and robustness to diverse object arrangements. Each policy model is evaluated across 30 predefined configurations per task. Evaluation results are averaged over these 30 configurations to summarize overall performance under varied conditions.

Baselines We compare WSA₁ with three representative and open-source embodied foundation models: π_0 [7], a generalist policy for continuous action prediction; $\pi_{0.5}$ [6], a policy for open-world robot control that demonstrates impressive generalization; and InternVLA-A1 [9], a unified model integrating visual understanding, video generation and action generation. For evaluation, we report the mean task success rate and the task progress score. The success rate measures whether the whole task is completed successfully, while the progress score reveals progress of full task execution.

Evaluation Results As shown in Table 3, WSA₁ achieves leading performance over baselines under real-world setting. Across 7 tabletop manipulation tasks, both WSA₁-B and WSA₁-L achieve an average success rate above 77% and an average completeness score exceeding 82%, substantially outperforming the second-best model $\pi_{0.5}$, which obtains 54.9% and 63.3%, respectively. Moreover, the improvement is consistent across both the single-arm PiPER and bimanual Lift2 platforms, with WSA₁ achieving the highest success rate on each task. These results highlight the effectiveness of the

Table 3: Real-world evaluation results on seven tabletop manipulation tasks. **SR** denotes the task success rate (%), and **C** denotes the task progress score (%).

Method	π_0		$\pi_{0.5}$		InternVLA-A1		WSA ₁ -B		WSA ₁ -L		
	VLA	3B	VLA	3B	WAM	3B	WSA	3B	WSA	6B	
<i>Evaluation Results on 7 Real-world Tabletop Robot Manipulation Tasks</i>											
Task Name	Robot Type	SR	C	SR	C	SR	C	SR	C	SR	C
RGB Block Sorting	AgileX Piper	70	70	70	70	50	50	80	80	83	83
Object Organization	AgileX Piper	50	50	77	77	37	37	80	80	77	77
Trash Cleaning	ARX Lift2	37	53	77	87	43	58	80	90	87	92
Pen Holder Placement	ARX Lift2	7	28	70	77	33	38	87	90	77	77
Toy Box Organization	ARX Lift2	13	18	13	27	37	48	60	72	70	85
Sweep Trash	ARX Lift2	29	40	26	44	44	78	79	89	85	93
Unzip Pencil Bag	ARX Lift2	30	43	55	63	25	43	75	75	85	90
<i>Average (%)</i>		33.8	43.2	54.9	63.3	39.2	51.3	77.5	82.7	80.3	86.5

Table 4: RoboTwin2.0 benchmark experimental results. WSA₁ is evaluated against closed-source and open-source embodied foundation models under hard setting. Mean success rate **SR** over 50 manipulation tasks is reported. WSA₁ achieves leading performance over open-sourced models.

Model Name	Access Status	Model Size	Model Type	SR (%)
Qwen-VLA [34]	Closed-source	5B	VLA	87.2
Being-H0.7 [26]	Closed-source	3B	WAM	89.6
MotuBrain [30]	Closed-source	-	WAM	96.1
π_0 [7]	Open-source	3B	VLA	58.4
$\pi_{0.5}$ [6]	Open-source	3B	VLA	76.8
ABot-M0 [40]	Open-source	4B	VLA	85.1
Motus [4]	Open-source	8B	WAM	87.0
InternVLA-A1 [9]	Open-source	3B	WAM	89.6
LingBot-VA [19]	Open-source	7B	WAM	91.5
Fast-WAM [44]	Open-source	6B	WAM	91.8
WSA₁-B	Open-source	3B	WSA	92.7
WSA₁-L	Open-source	6B	WSA	93.1

proposed WSA architecture. Rather than relying only on reactive 2D visual-action mapping, WSA₁ couples 3D-aligned visual thinking, 3D world dynamics, and 3D-conditioned action generation, leading to more reliable execution in spatially complex and long-horizon tasks.

4.3 Main Results on Simulation Benchmark

RoboTwin2.0 This is a challenging dual-arm manipulation benchmark that evaluates policy generalization under both clean and randomized environments. It covers diverse bimanual skills, including object handover, coordinated manipulation, spatially constrained interaction, and long-horizon tabletop tasks.

As shown in Table 4, WSA₁ achieves the best performance across open-source models, obtaining a success rate of 93% in the hard setting. Compared with large WAM models such as *Motus* and *Lingbot-VA* (model size > 3B), WSA₁-B with a model size of 3B delivers higher performance, and meanwhile remains competitive with the best closed-source model *MotuBrain*. As illustrated in Table 5, WSA₁ exhibits generalizable capability on long-horizon and spatially demanding tasks such as *Move Pillbottle Pad*, *Stack Blocks Three*, and *Open Microwave*. These results suggest that the proposed WSA paradigm is beneficial for learning transferable 3D world-action priors that support robust bimanual manipulation under diverse conditions.

Table 5: Comparison with state-of-the-art open-source models on RoboTwin2.0 under clean and randomized settings. Per-task success rate is reported.

Method	$\pi_{0.5}$ [6]		InternVLA-A1 [9]		Motus [4]		FastWAM [44]		WSA ₁ -B		WSA ₁ -L	
	VLA	3B	WAM	3B	WAM	8B	WAM	6B	WSA	3B	WSA	6B
<i>Evaluation Results on 50 Simulated Bimanual Robot Manipulation Tasks</i>												
Task Name	Clean	Rand.	Clean	Rand.	Clean	Rand.	Clean	Rand.	Clean	Rand.	Clean	Rand.
<i>Place Dual Shoes</i>	75	75	91	88	93	87	94	88	95	94	91	89
<i>Move Stapler Pad</i>	56	42	52	67	83	85	77	64	65	75	82	81
<i>Stack Blocks Two</i>	97	100	100	100	100	98	100	100	100	100	100	100
<i>Scan Object</i>	72	65	86	83	67	66	89	92	85	88	95	96
<i>Place Object Stand</i>	91	85	89	88	98	97	90	94	95	95	96	97
<i>Place Fan</i>	87	85	98	98	91	87	96	96	98	99	100	98
<i>Move Pillbottle Pad</i>	84	61	98	99	93	96	100	99	99	100	100	99
<i>Pick Dual Bottles</i>	93	63	92	87	96	90	100	96	94	89	98	96
<i>Blocks Ranking Rgb</i>	92	85	92	92	99	97	100	100	95	95	100	99
<i>..... (50 tasks)</i>												
<i>Turn Switch</i>	62	54	56	62	84	78	61	59	61	75	66	73
<i>Pick Diverse Bottles</i>	81	71	77	77	90	91	80	85	86	76	90	79
<i>Place Bread Basket</i>	77	64	90	91	91	94	91	93	99	94	98	97
<i>Stack Blocks Three</i>	91	76	90	93	91	95	95	97	98	98	99	100
<i>Put Bottles Dustbin</i>	84	79	90	93	81	79	95	90	95	92	92	98
<i>Place Can Basket</i>	62	62	81	72	81	76	71	69	80	79	81	80
<i>Stamp Seal</i>	79	55	75	75	93	92	90	94	73	82	75	89
<i>Hanging Mug</i>	18	17	31	47	38	38	58	62	50	50	40	42
<i>Handover Block</i>	66	57	90	73	86	73	95	81	91	84	96	85
<i>Stack Bowls Three</i>	77	71	89	90	79	87	80	81	92	93	91	91
<i>Place Object Basket</i>	80	76	89	87	81	87	89	88	84	87	91	90
<i>Open Microwave</i>	34	77	100	99	95	91	62	45	100	100	90	77
<i>Average (%)</i>	82.7	76.8	89.4	89.6	88.7	87.0	91.9	91.8	92.2	92.7	93.5	93.1

Table 6: Performance comparison on the LIBERO benchmark. Results are reported as success rates (%).

Method	LIBERO-Spatial	LIBERO-Object	LIBERO-Goal	LIBERO-10	Average
π_0 [7]		98.0	96.8	94.4	94.4
$\pi_{0.5}$ [6]		98.8	98.2	98.0	96.9
OpenVLA-OFT [17]		97.6	98.4	97.9	97.1
SpatialVLA [29]		88.2	89.9	78.6	78.1
GeoPredict [28]		98.0	98.2	95.7	96.5
Lingbot-VA [19]		98.5	99.6	97.2	98.5
DreamVLA [47]		97.5	94.0	89.5	92.6
Motus [4]		96.8	99.8	96.6	97.7
FastWAM [44]		98.2	100	97.0	97.6
WSA₁-B		98.6	99.6	97.2	97.4
WSA₁-L		99.4	99.8	98.0	98.2

LIBERO As reported in Table 6, WSA₁-B obtains 97.4% average success rate, surpassing representative VLA baselines. In addition, WSA₁-L further reaches 98.2% average success rate, achieving competitive results against all compared methods. Evaluation results across LIBERO-Spatial, LIBERO-Object, LIBERO-Goal, and LIBERO-10 suggest that WSA learns transferable spatial and action priors that generalize to diverse simulation tasks.

4.4 Ablation Study

In this section, we seek to answer the second question via two ablative experiments. First, we perform ablation studies to identify the contribution of world-spatial-action joint modeling, which involves three learning tasks: visual thinking, 3D world prediction and 3D action generation. Second, we study the effect of pre-training to reveal the details of full training process in WSA.

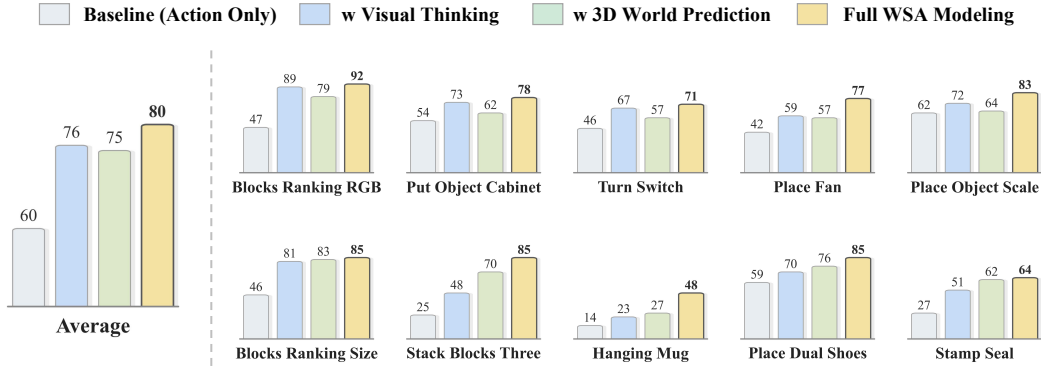


Figure 4: Investigation of WSA modeling on RoboTwin2.0 Benchmark.

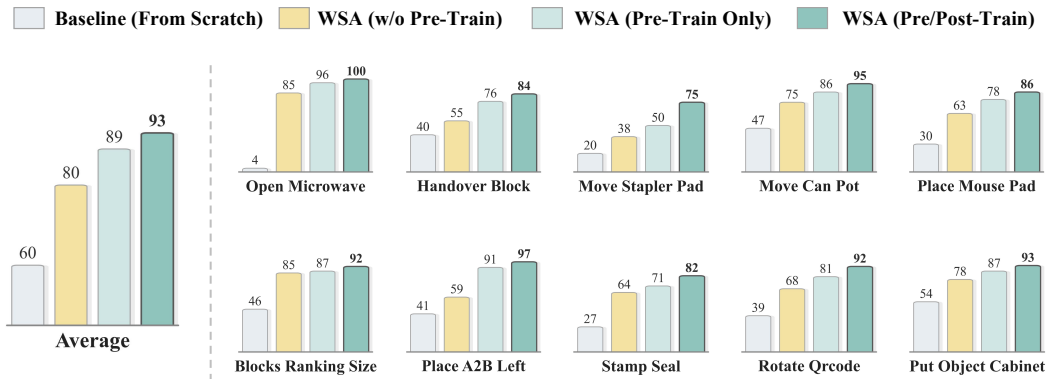


Figure 5: Ablation studies of WSA pre-training on RoboTwin2.0 Benchmark.

Investigation of WSA modeling We adopt the π -style VLA policy proposed in prior works [7, 6] as the baseline model, which integrates the pre-trained QWen3-VL-2B vision-language model [2] with a randomly initialized diffusion transformer serving as the action expert. All ablation experiments are conducted on the RoboTwin2.0 platform, and the corresponding results are presented in Figure 4. Specifically, the baseline model achieves a success rate (SR) of 60%. Notably, learning visual thinking improves the SR of action generation to 76%, while learning 3D world model yields a competitive SR of 75%. Full WSA modeling framework further outperforms all individual variants, reaching the best SR of 80%. Besides, modeling visual thinking is beneficial for manipulation tasks that rely heavily on visual semantics, object appearance, and temporally observable state changes, such as picking bottles and open microwave. In contrast, learning 3D world model improves contact-rich manipulation tasks such as rotate QR Code and stack blocks, which require a deep understanding of spatial geometry, object pose, and hand-object interaction. Based on the above observations, two key conclusions can be drawn. First, learning world dynamics in both 2D and 3D latent space is essential for generating generalized robot actions. Second, the bidirectional 3D world-action causal mechanism imposes effective constraints on action generation, thereby significantly enhancing the robustness of robot action learning.

The effect of pre-training To comprehensively investigate the efficacy of WSA pre-training, we design three comparative ablation settings: (1) WSA modeling is only applied in the post-training stage without pre-training on diverse heterogeneous robot datasets; (2) WSA modeling is adopted in the pre-training stage, while the post-training process only optimizes the action generation objective; (3) the model is consistently optimized with WSA modeling in both pre-training and post-training stages. As summarized in Figure 5, WSA pre-training delivers a substantial performance gain, increasing the SR from 80% to 89%. Moreover, applying WSA modeling in both pre-training and post-training further boosts the SR to 93%. These results demonstrate that WSA serves as an effective and essential training paradigm for building robust robot foundation models.

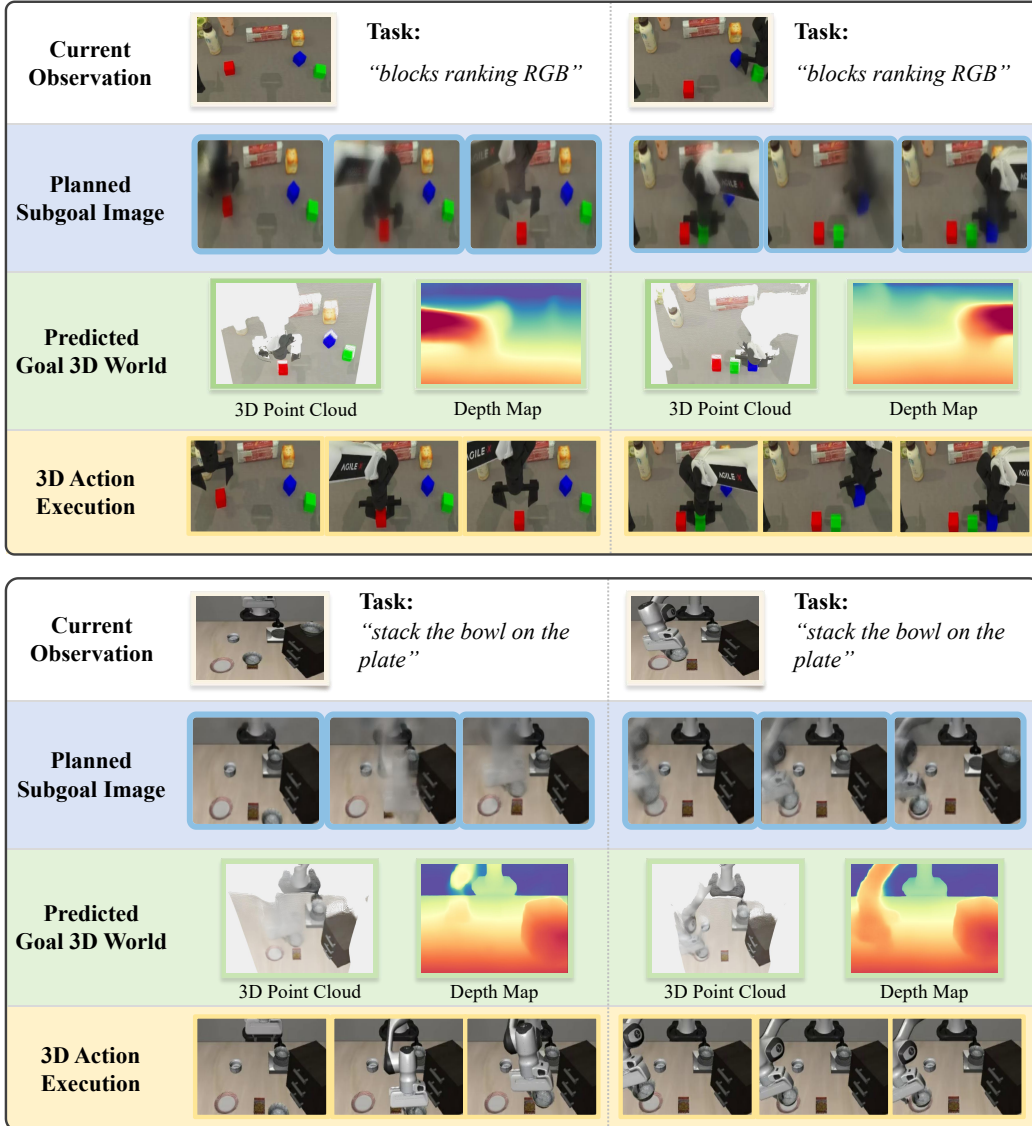


Figure 6: Visualization examples generated from WSA_1 . First row: robot’s observations with text instruction. Second row: generated subgoal images for visual planning. Third row: predicted 3D world that is rendered via Depth Anything model [21]. Fourth row: the real trajectory of executed actions.

4.5 Qualitative Analysis

To reveal how WSA_1 performs robot control, we present qualitative visualizations of the model’s predictions on various tasks. As illustrated in Figure 6, the visualization covers four views: visual observation with text instruction, predicted visual thought, goal 3D world prediction with 3D Gaussian and depth map, and trajectory of executed actions. From the results, we find that predicted visual plans well capture the task objective and well align the generated 3D world. Furthermore, driven by explicit 3D world modeling, the action trajectories are well-aligned with the predicted 3D goal states. These visual results demonstrate that WSA_1 unifies visual thinking, 3D world dynamics, and physical action generation within a shared latent space. It jointly models how actions alter the 3D world and how 3D world states guide action generation, thus leading to robust and generalizable manipulation behaviors.

5 Conclusion

This work addresses critical limitations of current robot foundation model paradigms, which lack understanding of 3D physical dynamics and bidirectional world–action causality. We propose the 3D-centric world-spatial-action joint modeling paradigm and instantiate WSA with two scales, i.e., WSA₁-B (3B) and WSA₁-L (6B). Built on Mixture-of-Transformers architecture, WSA models jointly learn 3D world-aware visual thinking, action-caused 3D world modeling, and 3D inverse dynamics modeling in a unified latent space. Each model is pre-trained with only 6,000 hours of demonstration data (1,000 hours from real robots), yet achieves strong performance across simulation and real-world benchmarks. Our work demonstrates that 3D-centric world-spatial-action joint modeling enables robots to learn transferable physical interaction priors, paving a practical and affordable path for generalizable robot foundation models.

References

- [1] Niket Agarwal, Arslan Ali, Maciej Bala, Yogesh Balaji, Erik Barker, Tiffany Cai, Prithvijit Chattopadhyay, Yongxin Chen, Yin Cui, Yifan Ding, Daniel Dworakowski, Jiaojiao Fan, Michele Fenzi, Francesco Ferroni, Sanja Fidler, Dieter Fox, Songwei Ge, Yunhao Ge, Jinwei Gu, Siddharth Gururani, Ethan He, Jiahui Huang, Jacob Huffman, Pooya Jannaty, Jingyi Jin, Seung Wook Kim, Gergely Klár, Grace Lam, Shiyi Lan, Laura Leal-Taixe, Anqi Li, Zhaoshuo Li, Chen-Hsuan Lin, Tsung-Yi Lin, Huan Ling, Ming-Yu Liu, Xian Liu, Alice Luo, Qianli Ma, Hanzi Mao, Kaichun Mo, Arsalan Mousavian, Seungjun Nah, Sriharsha Niverty, David Page, Despoina Paschalidou, Zeeshan Patel, Lindsey Pavao, Morteza Ramezani, Fitsum Reda, Xiaowei Ren, Vasanth Rao Naik Sabavat, Ed Schmerling, Stella Shi, Bartosz Stefaniak, Shitao Tang, Lyne Tchapmi, Przemek Tredak, Wei-Cheng Tseng, Jibin Varghese, Hao Wang, Haoxiang Wang, Heng Wang, Ting-Chun Wang, Fangyin Wei, Xinyue Wei, Jay Zhangjie Wu, Jiashu Xu, Wei Yang, Lin Yen-Chen, Xiaohui Zeng, Yu Zeng, Jing Zhang, Qinsheng Zhang, Yuxuan Zhang, Qingqing Zhao, and Artur Zolkowski. 2025. Cosmos world foundation model platform for physical ai. *arXiv preprint arXiv:2501.03575* (2025).
- [2] Shuai Bai, Yuxuan Cai, Ruizhe Chen, Keqin Chen, Xionghui Chen, Zesen Cheng, Lianghao Deng, Wei Ding, Chang Gao, Chunjiang Ge, et al. 2025. Qwen3-vl technical report. *arXiv preprint arXiv:2511.21631* (2025).
- [3] Shuai Bai, Keqin Chen, Xuejing Liu, Jialin Wang, Wenbin Ge, Sibao Song, Kai Dang, Peng Wang, Shijie Wang, Jun Tang, Humen Zhong, Yuanzhi Zhu, Mingkun Yang, Zhaohai Li, Jianqiang Wan, Pengfei Wang, Wei Ding, Zheren Fu, Yiheng Xu, Jiabo Ye, Xi Zhang, Tianbao Xie, Zesen Cheng, Hang Zhang, Zhibo Yang, Haiyang Xu, and Junyang Lin. 2025. Qwen2.5-VL Technical Report. *arXiv preprint arXiv:2502.13923* (2025).
- [4] Hongzhe Bi, Hengkai Tan, Shenghao Xie, Zeyuan Wang, Shuhe Huang, Haitian Liu, Ruowen Zhao, Yao Feng, Chendong Xiang, Yinze Rong, Hongyan Zhao, Hanyu Liu, Zhizhong Su, Lei Ma, Hang Su, and Jun Zhu. 2025. Motus: A Unified Latent Action World Model. *arXiv preprint arXiv:2512.13030* (2025).
- [5] Johan Bjorck, Fernando Castañeda, Nikita Cherniadev, Xingye Da, Runyu Ding, Linxi "Jim" Fan, Yu Fang, Dieter Fox, Fengyuan Hu, Spencer Huang, Joel Jang, Zhenyu Jiang, Jan Kautz, Kaushil Kundalia, Lawrence Lao, Zhiqi Li, Zongyu Lin, Kevin Lin, Guilin Liu, Edith Llonet, Loic Magne, Ajay Mandlekar, Avnish Narayan, Soroush Nasiriany, Scott Reed, You Liang Tan, Guanzhi Wang, Zu Wang, Jing Wang, Qi Wang, Jiannan Xiang, Yuqi Xie, Yinzen Xu, Zhenjia Xu, Seonghyeon Ye, Zhiding Yu, Ao Zhang, Hao Zhang, Yizhou Zhao, Ruijie Zheng, and Yuke Zhu. 2026. GR00T N1: An Open Foundation Model for Generalist Humanoid Robots. *arXiv preprint arXiv:2503.14734* (2026).
- [6] Kevin Black, Noah Brown, James Darpinian, Karan Dhabalia, Danny Driess, Adnan Esmail, Michael Robert Equi, Chelsea Finn, Niccolo Fusai, Manuel Y. Galliker, Dibya Ghosh, Lachy Groom, Karol Hausman, brian ichter, Szymon Jakubczak, Tim Jones, Liyiming Ke, Devin LeBlanc, Sergey Levine, Adrian Li-Bell, Mohith Mothukuri, Suraj Nair, Karl Pertsch, Allen Z. Ren, Lucy Xiaoyang Shi, Laura Smith, Jost Tobias Springenberg, Kyle Stachowicz, James Tanner, Quan Vuong, Homer Walke, Anna Walling, Haohuan Wang, Lili Yu, and Ury Zhilinsky.

2025. $\pi_{0.5}$: a Vision-Language-Action Model with Open-World Generalization. In *CoRL*, Vol. 305. 17–40.
- [7] Kevin Black, Noah Brown, Danny Driess, Adnan Esmail, Michael Equi, Chelsea Finn, Niccolo Fusai, Lachy Groom, Karol Hausman, Brian Ichter, Szymon Jakubczak, Tim Jones, Liyiming Ke, Sergey Levine, Adrian Li-Bell, Mohith Mothukuri, Suraj Nair, Karl Pertsch, Lucy Xiaoyang Shi, James Tanner, Quan Vuong, Anna Walling, Haohuan Wang, and Ury Zhilinsky. 2024. π_0 : A Vision-Language-Action Flow Model for General Robot Control. *arXiv preprint arXiv:2410.24164* (2024).
- [8] Qingwen Bu, Jisong Cai, Li Chen, Xiuqi Cui, Yan Ding, Siyuan Feng, Shenyuan Gao, Xindong He, Xuan Hu, Xu Huang, et al. 2025. Agibot world colosseo: A large-scale manipulation platform for scalable and intelligent embodied systems. *arXiv preprint arXiv:2503.06669* (2025).
- [9] Junhao Cai, Zetao Cai, Jiafei Cao, Yilun Chen, Zeyu He, Lei Jiang, Hang Li, Hengjie Li, Yang Li, Yufei Liu, et al. 2026. InternVLA-A1: Unifying Understanding, Generation and Action for Robotic Manipulation. *arXiv preprint arXiv:2601.02456* (2026).
- [10] Tianxing Chen, Zanzin Chen, Baijun Chen, Zijian Cai, Yibin Liu, Zixuan Li, Qiwei Liang, Xianliang Lin, Yiheng Ge, Zhenyu Gu, Weiliang Deng, Yubin Guo, Tian Nian, Xuanbing Xie, Qiangyu Chen, Kailun Su, Tianling Xu, Guodong Liu, Mengkang Hu, Huan ang Gao, Kaixuan Wang, Zhixuan Liang, Yusen Qin, Xiaokang Yang, Ping Luo, and Yao Mu. 2025. RoboTwin 2.0: A Scalable Data Generator and Benchmark with Strong Domain Randomization for Robust Bimanual Robotic Manipulation. *arXiv preprint arXiv:2506.18088* (2025).
- [11] Zhe Chen, Jiannan Wu, Wenhai Wang, Weijie Su, Guo Chen, Sen Xing, Muyan Zhong, Qinglong Zhang, Xizhou Zhu, Lewei Lu, et al. 2024. Internvl: Scaling up vision foundation models and aligning for generic visual-linguistic tasks. In *CVPR*. 24185–24198.
- [12] Andy Clark. 2013. Whatever next? Predictive brains, situated agents, and the future of cognitive science. *Behavioral and brain sciences* 36, 3 (2013), 181–204.
- [13] Howard Gardner. 2011. *Frames of Mind: The Theory of Multiple Intelligences*. Basic Books, New York.
- [14] Ryan Hoque, Peide Huang, David J. Yoon, Mouli Sivapurapu, and Jian Zhang. 2025. EgoDex: Learning Dexterous Manipulation from Large-Scale Egocentric Video. *arXiv preprint arXiv:2505.11709* (2025).
- [15] Wenlong Huang, Yu-Wei Chao, Afsar Mousavian, Ming-Yu Liu, Dieter Fox, Kaichun Mo, and Li Fei-Fei. 2026. PointWorld: Scaling 3D World Models for In-The-Wild Robotic Manipulation. In *CVPR*.
- [16] Moo Jin Kim, Yihuai Gao, Tsung-Yi Lin, Yen-Chen Lin, Yunhao Ge, Grace Lam, Percy Liang, Shuran Song, Ming-Yu Liu, Chelsea Finn, and Jinwei Gu. 2026. Cosmos Policy: Fine-Tuning Video Models for Visuomotor Control and Planning. *arXiv preprint arXiv:2601.16163* (2026).
- [17] Moo Jin Kim, Karl Pertsch, Siddharth Karamcheti, Ted Xiao, Ashwin Balakrishna, Suraj Nair, Rafael Rafailov, Ethan P Foster, Pannag R Sanketi, Quan Vuong, Thomas Kollar, Benjamin Burchfiel, Russ Tedrake, Dorsa Sadigh, Sergey Levine, Percy Liang, and Chelsea Finn. 2025. OpenVLA: An Open-Source Vision-Language-Action Model. In *CoRL*, Vol. 270. 2679–2713.
- [18] Stephen M Kosslyn. 1996. *Image and brain: The resolution of the imagery debate*. MIT press.
- [19] Lin Li, Qihang Zhang, Yiming Luo, Shuai Yang, Ruilin Wang, Fei Han, Mingrui Yu, Zelin Gao, Nan Xue, Xing Zhu, Yujun Shen, and Yinghao Xu. 2026. Causal World Modeling for Robot Control. *arXiv preprint arXiv:2601.21998* (2026).
- [20] Peiyan Li, Yixiang Chen, Yuan Xu, Jiabing Yang, Xiangnan Wu, Jun Guo, Nan Sun, Long Qian, Xinghang Li, Xin Xiao, Jing Liu, Nianfeng Liu, Tao Kong, Yan Huang, Liang Wang, and Tieniu Tan. 2026. Multi-View Video Diffusion Policy: A 3D Spatio-Temporal-Aware Video Action Model. *arXiv preprint arXiv:2604.03181* (2026).

- [21] Haotong Lin, Sili Chen, Junhao Liew, Donny Y Chen, Zhenyu Li, Guang Shi, Jiashi Feng, and Bingyi Kang. 2025. Depth anything 3: Recovering the visual space from any views. *arXiv preprint arXiv:2511.10647* (2025).
- [22] Yaron Lipman, Ricky TQ Chen, Heli Ben-Hamu, Maximilian Nickel, and Matt Le. 2022. Flow matching for generative modeling. In *ICLR*.
- [23] Bo Liu, Yifeng Zhu, Chongkai Gao, Yihao Feng, Qiang Liu, Yuke Zhu, and Peter Stone. 2023. LIBERO: benchmarking knowledge transfer for lifelong robot learning. In *NeurIPS*.
- [24] Songming Liu, Lingxuan Wu, Bangguo Li, Hengkai Tan, Huayu Chen, Zhengyi Wang, Ke Xu, Hang Su, and Jun Zhu. 2025. RDT-1B: a Diffusion Foundation Model for Bimanual Manipulation. In *ICLR*, Vol. 2025. 29982–30009.
- [25] Yunfan Lou, Xiaowei Chi, Xiaojie Zhang, Zezhong Qian, Chengxuan Li, Rongyu Zhang, Yaoxu Lyu, Guoyu Song, Chuyao Fu, Haoxuan Xu, Pengwei Wang, and Shanghang Zhang. 2026. Mask World Model: Predicting What Matters for Robust Robot Policy Learning. *arXiv preprint arXiv:2604.19683* (2026).
- [26] Hao Luo, Wanpeng Zhang, Yicheng Feng, Sipeng Zheng, Haiweng Xu, Chaoyi Xu, Ziheng Xi, Yuhui Fu, and Zongqing Lu. 2026. Being-H0.7: A Latent World-Action Model from Egocentric Videos. *arXiv preprint arXiv:2605.00078* (2026).
- [27] Jonas Pai, Liam Achenbach, Victoriano Montesinos, Benedek Forrai, Oier Mees, and Elvis Nava. 2025. mimic-video: Video-Action Models for Generalizable Robot Control Beyond VLAs. *arXiv preprint 2512.15692* (2025).
- [28] Jingjing Qian, Boyao Han, Chen Shi, Lei Xiao, Long Yang, Shaoshuai Shi, and Li Jiang. 2025. GeoPredict: Leveraging Predictive Kinematics and 3D Gaussian Geometry for Precise VLA Manipulation. In *CVPR*.
- [29] Delin Qu, Zeren Gu, Bin Zhao, Dong Wang, and Xuelong Li. 2025. SpatialVLv1a:3DVLAA: Exploring Spatial Representations for Visual-Language-Action Models. In *Robotics: Science and Systems (RSS)*.
- [30] MotuBrain Team, Chendong Xiang, Fan Bao, Haitian Liu, Hengkai Tan, Hongzhe Bi, James Li, Jiabao Liu, Jingrui Pang, Kiro Jing, Louis Liu, Mengchen Cai, Rongxu Cui, Ruowen Zhao, Runqing Wang, Shuhe Huang, Yao Feng, Yinze Rong, Zeyuan Wang, and Jun Zhu. 2026. MotuBrain: An Advanced World Action Model for Robot Control. *arXiv preprint arXiv:2604.27792* (2026).
- [31] Octo Model Team, Dibya Ghosh, Homer Walke, Karl Pertsch, Kevin Black, Oier Mees, Sudeep Dasari, Joey Hejna, Tobias Kreiman, Charles Xu, Jianlan Luo, You Liang Tan, Lawrence Yunliang Chen, Pannag Sanketi, Quan Vuong, Ted Xiao, Dorsa Sadigh, Chelsea Finn, and Sergey Levine. 2024. Octo: An Open-Source Generalist Robot Policy. *arXiv preprint arXiv:2405.12213* (2024).
- [32] Team Wan, Ang Wang, Baole Ai, Bin Wen, Chaojie Mao, Chen-Wei Xie, Di Chen, Feiwei Yu, Haiming Zhao, Jianxiao Yang, Jianyuan Zeng, Jiayu Wang, Jingfeng Zhang, Jingren Zhou, Jinkai Wang, Jixuan Chen, Kai Zhu, Kang Zhao, Keyu Yan, Lianghua Huang, Mengyang Feng, Ningyi Zhang, Pandeng Li, Pingyu Wu, Ruihang Chu, Ruili Feng, Shiwei Zhang, Siyang Sun, Tao Fang, Tianxing Wang, et al. 2025. Wan: Open and Advanced Large-Scale Video Generative Models. *arXiv preprint arXiv:2503.20314* (2025).
- [33] Yang Tian, Yuyin Yang, Yiman Xie, Zetao Cai, Xu Shi, Ning Gao, Hangxu Liu, Xuekun Jiang, Zherui Qiu, Feng Yuan, et al. 2025. Interndata-a1: Pioneering high-fidelity synthetic data for pre-training generalist policy. *arXiv preprint arXiv:2511.16651* (2025).
- [34] Qiuyue Wang, Mingsheng Li, Jian Guan, Jinhui Ye, Sicheng Xie, Yitao Liu, Junhao Chen, Zhixuan Liang, Jie Zhang, Xintong Hu, Xuhong Huang, Pei Lin, Junyang Lin, Dayiheng Liu, Shuai Bai, Jingren Zhou, Jiazhao Zhang, Haoqi Yuan, Gengze Zhou, Hang Yin, Ye Wang, Yiyang Huang, Zixing Lei, Wujian Peng, Delin Chen, Yingming Zheng, Jingyang Fan, Xianwei Zhuang, Xin Zhou, Haoyang Li, Anzhe Chen, Tong Zhang, Xuejing Liu, Yuchong

- Sun, Ruizhe Chen, Zhaohai Li, Chenxu Lü, Zhibo Yang, Tao Yu, and Xionghui Chen. 2026. Qwen-VLA: Unifying Vision-Language-Action Modeling across Tasks, Environments, and Robot Embodiments. *arXiv preprint arXiv:2605.30280* (2026).
- [35] Xuanhan Wang, Huimin Deng, Lianli Gao, and Jingkuan Song. 2025. Scale-Aware Pre-Training for Human-Centric Visual Perception: Enabling Lightweight and Generalizable Models. *arXiv preprint arXiv:2503.08201* (2025).
- [36] Junjie Wen, Yichen Zhu, Jinming Li, Zhibin Tang, Chaomin Shen, and Feifei Feng. 2025. DexVLA: Vision-Language Model with Plug-In Diffusion Expert for General Robot Control. In *CoRL*.
- [37] Daniel M Wolpert and Zoubin Ghahramani. 2000. Computational principles of movement neuroscience. *Nature neuroscience* 3, 11 (2000), 1212–1217.
- [38] Adina Yakefu, Bin Xie, Chongyang Xu, Enwen Zhang, Erjin Zhou, Fan Jia, Haitao Yang, Haoqiang Fan, Haowei Zhang, Hongyang Peng, et al. 2025. RoboChallenge: Large-scale Real-robot Evaluation of Embodied Policies. *arXiv preprint arXiv:2510.17950* (2025).
- [39] Ruihan Yang, Qinxi Yu, Yecheng Wu, Rui Yan, Borui Li, An-Chieh Cheng, Xueyan Zou, Yunhao Fang, Xuxin Cheng, Ri-Zhao Qiu, Hongxu Yin, Sifei Liu, Song Han, Yao Lu, and Xiaolong Wang. 2025. EgoVLA: Learning Vision-Language-Action Models from Egocentric Human Videos. *arXiv preprint arXiv:2507.12440* (2025).
- [40] Yandan Yang, Shuang Zeng, Tong Lin, Xinyuan Chang, Dekang Qi, Junjin Xiao, Haoyun Liu, Ronghan Chen, Yuzhi Chen, Dongjie Huo, Feng Xiong, Xing Wei, Zhiheng Ma, and Mu Xu. 2026. ABot-M0: VLA Foundation Model for Robotic Manipulation with Action Manifold Learning. *arXiv preprint arXiv:2602.11236* (2026).
- [41] Seonghyeon Ye, Yunhao Ge, Kaiyuan Zheng, Shen Yuan Gao, Sihyun Yu, George Kurian, Suneel Indupuru, You Liang Tan, Chuning Zhu, Jiannan Xiang, Ayaan Malik, Kyungmin Lee, William Liang, Nadun Ranawaka, Jiasheng Gu, Yinzhen Xu, Guanzhi Wang, Fengyuan Hu, Avnish Narayan, Johan Bjorck, Jing Wang, Gwanghyun Kim, Dantong Niu, Ruijie Zheng, Yuqi Xie, Jimmy Wu, Qi Wang, Ryan Julian, Danfei Xu, Yilun Du, Yevgen Chebotar, Scott Reed, Jan Kautz, Yuke Zhu, Linxi "Jim" Fan, and Joel Jang. 2026. World Action Models are Zero-shot Policies. *arXiv preprint arXiv:2602.15922* (2026).
- [42] Zhenhan Yin, Xuanhan Wang, Jiahao Jiang, Kaiyuan Deng, Pengqi Chen, Shuangle Li, Chong Liu, Xing Xu, Jingkuan Song, Lianli Gao, and Heng Tao Shen. 2026. MiVLA: Towards Generalizable Vision-Language-Action Model with Human-Robot Mutual Imitation Pre-training. In *Proceedings of the IEEE/CVF Conference on Computer Vision and Pattern Recognition (CVPR) Findings*. 1535–1545.
- [43] Zhaoshu Yu, Bo Wang, Pengpeng Zeng, Haonan Zhang, Ji Zhang, Zheng Wang, Lianli Gao, Jingkuan Song, Nicu Sebe, and Heng Tao Shen. 2025. A survey on efficient vision-language-action models. *arXiv preprint arXiv:2510.24795* (2025).
- [44] Tianyuan Yuan, Zibin Dong, Yicheng Liu, and Hang Zhao. 2026. Fast-WAM: Do World Action Models Need Test-time Future Imagination? *arXiv preprint arXiv:2603.16666* (2026).
- [45] Xiaohua Zhai, Basil Mustafa, Alexander Kolesnikov, and Lucas Beyer. 2023. Sigmoid Loss for Language Image Pre-Training. In *ICCV*. 11975–11986.
- [46] Peng-Fei Zhang, Ying Cheng, Xiaofan Sun, Shijie Wang, Fengling Li, Lei Zhu, and Heng Tao Shen. 2025. A step toward world models: A survey on robotic manipulation. *arXiv preprint arXiv:2511.02097* (2025).
- [47] Wenyao Zhang, Hongsi Liu, Zekun Qi, Yunnan Wang, Xinqiang Yu, Jiazhao Zhang, Runpei Dong, Jiawei He, Fan Lu, He Wang, Zhizheng Zhang, Li Yi, Wenjun Zeng, and Xin Jin. 2025. DreamVLA: A Vision-Language-Action Model Dreamed with Comprehensive World Knowledge. In *NeurIPS*.

- [48] Qingqing Zhao, Yao Lu, Moo Jin Kim, Zipeng Fu, Zhuoyang Zhang, Yecheng Wu, Zhaoshuo Li, Qianli Ma, Song Han, Chelsea Finn, Ankur Handa, Tsung-Yi Lin, Gordon Wetzstein, Ming-Yu Liu, and Donglai Xiang. 2025. CoT-VLA: Visual Chain-of-Thought Reasoning for Vision-Language-Action Models. In *CVPR*. 1702–1713.
- [49] Haoyu Zhen, Xiaowen Qiu, Peihao Chen, Jincheng Yang, Xin Yan, Yilun Du, Yining Hong, and Chuang Gan. 2024. 3D-VLA: A 3D Vision-Language-Action Generative World Model. 61229–61245.
- [50] Brianna Zitkovich, Tianhe Yu, Sichun Xu, Peng Xu, Ted Xiao, Fei Xia, Jialin Wu, Paul Wohlhart, Stefan Welker, Ayzaan Wahid, Quan Vuong, Vincent Vanhoucke, Huong Tran, Radu Soricut, Anikait Singh, Jaspiar Singh, Pierre Sermanet, Pannag R. Sanketi, Grecia Salazar, Michael S. Ryoo, Krista Reymann, Kanishka Rao, Karl Pertsch, Igor Mordatch, Henryk Michalewski, Yao Lu, Sergey Levine, Lisa Lee, Tsang-Wei Edward Lee, Isabel Leal, Yuheng Kuang, Dmitry Kalashnikov, Ryan Julian, Nikhil J. Joshi, Alex Irpan, Brian Ichter, Jasmine Hsu, Alexander Herzog, Karol Hausman, Keerthana Gopalakrishnan, Chuyuan Fu, Pete Florence, Chelsea Finn, Kumar Avinava Dubey, Danny Driess, Tianli Ding, Krzysztof Marcin Choromanski, Xi Chen, Yevgen Chebotar, Justice Carbajal, Noah Brown, Anthony Brohan, Montserrat Gonzalez Arenas, and Kehang Han. 2023. RT-2: Vision-Language-Action Models Transfer Web Knowledge to Robotic Control. In *CoRL*, Vol. 229. 2165–2183.